ization functions,[2] it is evident that the calculations at the 6-31G** level predict a bent structure for the B-H-B bond.[7] This discrepancy with former results could be attributed to the different optimization techniques used.

As seen from Table I, the 6-31** basis set calculations assign a 149.9° value to the $B_1-H_1-B_2$ angle and show a slight asymmetry for the B_1-H_1 and B_2-H_1 bond, which feature a 0.02-Å difference in bond length. The B-H bonds where the hydrogen atom is *not* the bridge do not feature significant differences; however, they are all smaller than the central B-H bond. The same effect was found and discussed for the aluminum compound.[4]

The asymmetry mentioned above can be attributed, by using a resonance approach, to the contribution of the structure featuring the BH_4^- anion as a whole donating some of its charge to the electron-deficient BH_3, yielding the $BH_4^-\cdot BH_3$ entity.

As seen from Table I and Figure 1a, the anion features C_s symmetry, with the H_3 and H_5 atoms set in the plane of the B1,H1,B2 atoms. The optimized C_{2v} structure is found by us to feature a slightly higher energy than the C_s structure (0.3 kcal/mol). The preference for a bent structure of some bridged metallic compounds has been explained by a certain amount of bonding occurring between the metals.[6] In the $Al_2H_7^-$ anion, no such bonding takes place and, as a result, the central Al-H-Al bond assumes a linear structure. Since a split-valence basis set without polarization functions proved unreliable in the boron case, the 3-21G results for aluminum[4] could be questioned, but since the X-ray data experiments have been confirmed, it seems safe to assume them to be correct.

An explanation for the different structure of the $B_2H_7^-$ and $Al_2H_7^-$ anions could be found in the higher electronegativity of boron and in the higher metallicity of aluminium, which would lead to a larger positive charge accumulation on the aluminium atoms and consequently a greater repulsion between them, favoring a linear Al-H-L bond. When the Mulliken overlap population is examined, the B-B region shows a 0.03-eu charge in the 6-31G** level calculations, indicative of a slight B-B bonding, while in the calculations carried out on the bent B-H-B bond with the 6-31G basis set, the B-B overlap is of only 0.01 eu. The reason for this difference can be found by examining the composition of the molecular orbitals. Upon such examination, one notices a small bonding participation by the d orbitals on the borons to be present in the ninth MO (HOMO) as well as in the seventh occupied MO. We also considered another possible explanation for the bent structure, by the examination of molecular orbitals related to the central hydrogen-boron bond. Those are the third and seventh MO's. In both of them, as expected, the largest contribution is provided by the 1s hydrogen atomic orbitals. As far as the boron atoms are concerned, in the third MO their 2s orbital contribute the most, while in the seventh MO the greatest contribution belongs to the p_y orbitals (y being the B-B axis). One notices, though, a mixing of the p_x orbital of the hydrogen (x being the axis perpendicular to the B-B bond and contained in the B-H-B plane) in the third orbital. The p_x orbital of hydrogen participates also in the seventh MO, and in both cases, it is of a bonding nature, providing additional stabilization for a bent structure. This effect might be contributing factor to the bending of the B-H-B linkage, but not the essential one. Indeed, as shown by Schleyer et al.[7] the 6-31G* basis set calculations also predict a bent structure for the anion, thus proving that the addition of p orbitals on the hydrogen is not mandatory.

(7) A simultaneous study by K. Raghavachari, P. v. R. Schleyer, G. W. Spitznagel, and J. A. Pople reaches the same conclusions, with the use of the 6-31G** and MP2 calculations. The MP2 term modifies only slightly the geometry of the anion.

The results obtained for the geometry of the $B_2H_6F^-$ anion show more clearly the importance of occupied p orbitals in producing a nonlinear structure. Indeed, the results show beyond any doubt a bent B-F-B central linkage, both through the use of 6-31G and 6-31G** basis sets. It is evident in this case that the increased stabilization that occurs for a molecular orbital of a_1 asymmetry (C_{2v}) upon bending supersedes the repulsion between the borons, which in the $B_2H_6F^-$ anion features a positive charge of about 0.5 eu and, as such, is much higher than the 0.2 eu present in the B_2H_7 anion.

In conclusion, the $B_2H_7^-$ structure, as described by the 6-31G** basis set, features a bent B-H-B central linkage, in agreement with the X-ray data of Shore et al.[1] However, there are differences between the experimental findings[1] and the theoretical results: the difference between B_1-H_1 and B_2-H_2 is only 0.02 Å in this work while the experimental result shows a 1.27-Å difference. Also, the $B_1-H_1-B_2$ angle is slightly larger according to our calculations (150° vs. the experimental 136°). The theoretical model also features a larger B_1-B_2 distance than the experimental boron-boron distance. The main issue, though, is the fact that theoretical Hartree-Fock calculations with a 6-31G** basis set predict a bent structure for the anion. We find however the energetic advantage of the bent structure over the linear one to be quite small (below 1 kcal/mol). This is in agreement with the results of Schleyer et al.[7] who also find a small value for the energy difference of the two species.

Registry No. $B_2H_7^-$, 27380-11-6; $B_2H_6F^-$, 82630-61-3.

Contribution from The Institute of Scientific and Industrial Research, Osaka University, Ibaraki, Osaka 567, Japan

High-Pressure Synthesis and Magnetic Properties of MMnSb (M = Ti, V, Cr) with Ni_2In Type Structures

Y. Noda,† M. Shimada,* and M. Koizumi

Received March 30, 1983

Pnictides with a chemical formula of MM'X (M and M' are 3d transition metals) are intermetallic compounds, and concepts of classical valency are not easily applied to them. Although most of these compounds are metallic, they exhibit a variety of magnetic properties such as ferromagnetism, ferrimagnetism, antiferromagnetism, and Pauli paramagnetism. Unlike the phosphides and arsenides, systematic investigations of antimonides have rarely been carried out.[1] Figure 1 shows the crystal structures of the MM'Sb compounds previously synthesized.[2-4] As seen in this figure, all of them except for CoNiSb and Mn_2Sb take a MgCuSb (Cl_b) type structure. Since the MgCuSb and the Ni_2In type structures are not found in the phosphides and arsenides,[5] it is expected that there exists a discontinuity in crystal structure between arsenides and antimonides. We have tried to synthesize antimonides in order to increase our understanding of the crystal structures and magnetic properties that they exhibit. During our synthetic studies of antimonides, it was found that high-pressure transformation of VCoSb and VFeSb from the MgCuSb type structure to the Ni_2In type structure occurred under high temperature-pressure conditions.[6]

In this study, new antimonides of TiMnSb, VMnSb, and CrMnSb with the Ni_2In type structure were synthesized under high temperature-pressure conditions and their magnetic properties were examined.

† Present address: Central Laboratory of KDD, Meguro-ku, Tokyo 153.

0020-1669/84/1323-0628$01.50/0

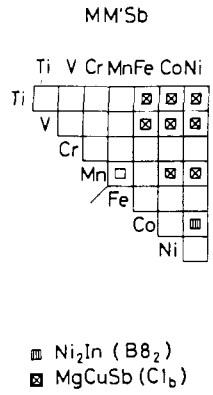

Figure 1. Crystal structure of the antimonides MM'Sb.

Table I. Crystallographic Parameters

compd	a/nm	c/nm	$V/10^{-3}$ nm^3	c/a
TiMnSb	0.4386	0.5820	96.97	1.327
VMnSb	0.4317	0.5586	90.16	1.294
CrMnSb	0.4292	0.5623	89.71	1.310
VFeSb-II(6)	0.4233	0.5398	83.77	1.275
VCoSb-II(6)	0.4200	0.5398	82.46	1.285

Experimental Section

Starting materials of MMnSb (M = Ti, V, Cr) were prepared by mixing titanium (99.99%), vanadium (99.9%), chromium (99.9%), manganese (99.9%), and antimony (99.99%) powders in the desired ratios. The powders were put into a cylindrical BN capsule, which was placed in a carbon heater. The assemblage was put into a pyrophyllite cube. The cube was subjected to high temperature–pressure conditions with use of a cubic anvil type apparatus.[6] The magnitude of pressure inside the cell was calibrated on the basis of the electrical transition of Bi (2.55 GPa) and Ba (5.5 GPa). The temperature of the sample was measured by a Pt–Pt/13% Rh thermocouple in the center of the cube. The reaction was carried out at 5.0 GPa and 900 °C for 1 h. The sample was quenched to room temperature prior to the release of applied pressure. Products were identified by X-ray diffraction with Ni-filtered Cu Kα radiation. Lattice constants were determined by a least-squares method from high-angle powder patterns. Silicon was used as an internal standard. Magnetic measurements were performed by using a magnetic torsion balance in the temperature range 5–350 K in a field of 12 kOe.

Results and Discussion

X-ray diffraction patterns for all samples of TiMnSb, VMnSb, and CrMnSb synthesized under high temperature–pressure conditions were completely indexed as the hexagonal Ni_2In type structure, and no other phases were found. The crystallographic parameters of these three compounds are listed in Table I. It is expected that in this structure the Ti, V, Cr, and Mn atoms are randomly distributed on both 2(a) and 2(d) sites and that the Sb atoms occupy the 2(c) site as discussed in our previous report.[6] The only other antimonides with the Ni_2In type structure that have been reported are CoNiSb[7] and high-pressure phases of VCoSb and VFeSb.[6] Unit cell volumes of the antimonides MM'Sb with the Ni_2In type structure were examined in comparison with those of compounds MSb having the NiAs type structure. Figure 2 shows a unit cell volume (V) vs. $r_M^3 + r_{M'}^3$ plot for the MM'Sb compounds and a V vs. r_M^3 plot for the MSb compounds. In the present calculation, the metallic radii with 12-coordination numbers were adopted.[8] According to the Laves–Parthé model,[9,10] in the case of antimonides MM'Sb, the volume per formula is written as follows by using a metallic radius:

$$V = \frac{4\pi}{3\phi}[k(r_M^3 + r_{M'}^3) + lr_{Sb}^3]$$

where ϕ is the space-filling factor and k and l are size coefficients for the metal and metalloid atoms. Since a good linear relationship was recognized, as seen in Figure 2, the space-filling factors were determined to be 0.798 for MM'Sb compounds with the Ni_2In type structure and 0.541 for MSb compounds with the NiAs type structure.

The temperature dependence of the magnetic susceptibility of VMnSb is shown in Figure 3. VMnSb was antiferromganetic with a Néel temperature of 25 K and a paramagnetic

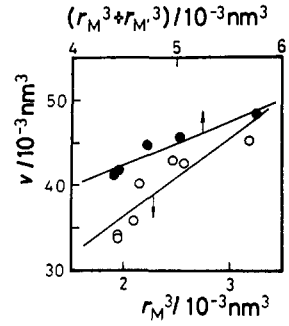

Figure 2. Relationship between formula volume and cubic metallic radius for MSb (open circles) and MM'Sb (solid circles).

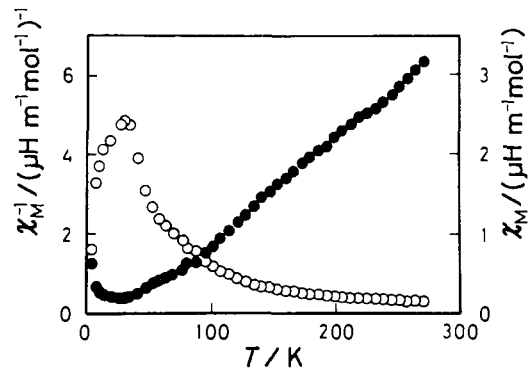

Figure 3. Magnetic susceptibility (open circles) and reciprocal magnetic susceptibility (solid circles) as a function of temperature for VMnSb.

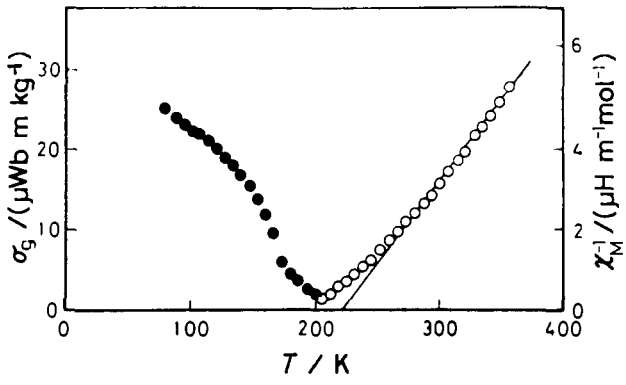

Figure 4. Magnetization (solid circles) and reciprocal magnetic susceptibility (open circles) as a function of temperature for CrMnSb.

(1) Goodenough, J. B. *J. Solid State Chem.* **1973**, *7*, 428.
(2) Kripyakevich, P. I.; Markiv, V. Ya. *Dopov. Akad. Nauk Ukr. RSR* **1963**, *12*, 1606.
(3) Nateva, M. G.; Murthy, M. R. L. N.; Begum, R. J.; Murthy, N. S. *Phys. Status Solidi A* **1970**, *3*, 959.
(4) Forster, R. H.; Jousto, G. B. *J. Phys. Chem. Solids* **1968**, *29*, 855.
(5) Roy-Montreuil, M.; Deyris, B.; Michel, A.; Rouault, A.; L'Hertier, P.; Nylund, A.; Senateur, J. P.; Fruchart, R. *Mat. Res. Stand.* **1972**, *7*, 813.
(6) Noda, Y.; Shimada, M.; M. Koizumi, M. *Inorg. Chem.* **1979**, *18*, 3244.
(7) Castellitz, L., *Monatsh. Chem.* **1952**, *83*, 1314.
(8) Wells, A. F. "Structure Inorganic Chemistry"; Clarendon Press: Oxford, 1975.
(9) Laves, F. "Theory of Alloy Phase"; American Society for Metals: Cleveland, OH, 1956; p 124.
(10) Parthe, E. *Z. Kristallogr.* **1961**, *115*, 52.

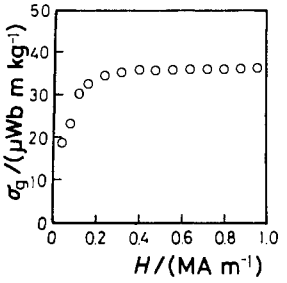

Figure 5. Magnetic field dependence of magnetization for CrMnSb at 77 K.

Table II. Magnetic Parameters

compd	T_c or T_N/K	θ_p/K	n_p/μ_B	n_F/μ_B
TiMnSb		−30	2.13	
VMnSb	25[a]	34	4.37	
CrMnSb	198[b]	223	3.50	1.17

[a] T_N. [b] T_c.

Curie temperature of 34 K. Since the sample obeyed the Curie–Weiss law in the paramagnetic region, the effective Bohr magneton per formula was calculated to be 4.37 μ_B. On the other hand, the compound CrMnSb was ferromagnetic with a Curie temperature of 198 K as shown in Figure 4. Since the paramagnetic Curie temperature had a positive value of 223 K, it is expected that the dominant magnetic interaction in CrMnSb was ferromagnetic. The field dependence of the magnetization at 77 K is shown in Figure 5. It is seen that the magnetization saturated at 320 kA m^{-1} (4.0 kOe) and the ferromagnetic moment per formula was calculated to be 1.17. No magnetic ordering of TiMnSb was found down to 10 K, and the effective Bohr magneton per formula was calculated to be 2.13 μ_B from the slope of a χ_M^{-1}–T curve. The magnetic parameters of these three compounds are tabulated in Table II. Although the MMnSb compounds contained twice as many transition-metal atoms per formula unit as the MSb compounds with the NiAs type structure, values of n_p of the former were not larger than those of the latter.[1] The magnetic properties of the present three compounds were different from each other. It is believed that these facts can be explained by a schematic 3d band model on the basis of that of MSb compounds with the NiAs type structure proposed by Goodenough,[1] but the detailed results have not yet been examined.

Registry No. TiMnSb, 88430-85-7; VMnSb, 88430-86-8; CrMnSb, 87716-72-1.

Contribution from the Department of Chemistry, University of Nottingham, Nottingham NG7 2RD, England

Photochemistry in Liquid Krypton: Generation and Thermal Stability of $Fe(CO)(N_2)(NO)_2$ and $Fe(N_2)_2(NO)_2$

Gerard E. Gadd, Martyn Poliakoff,* and James J. Turner*

Received July 5, 1983

We have recently demonstrated the value of noble gases as low-temperature solvents for both synthetic[1] (e.g., $Cr(CO)_{6-x}(N_2)_x$) and mechanisitic studies[2] ($Ni(CO)_3N_2 \xrightarrow{CO}$ $Ni(CO)_4$) of unstable species. There has long been interest[3] in the kinetics of ligand substitution in the isoelectronic series $Ni(CO)_4$, $Co(CO)_3NO$, and $Fe(CO)_2(NO)_2$. It therefore seemed appropriate in light of our $Ni(CO)_3N_2$ experiments[2] to investigate the generation and thermal stability of $Fe(CO)(N_2)(NO)_2$ and $Fe(N_2)_2(NO)_2$, particularly as Crichton and Rest have identified these presumably unstable species by photolysis of $Fe(CO)_2(NO)_2$ in solid N_2 matrices[4] at 10 K. This note summarizes our results.

Figure 1 shows IR spectra illustrating the photolysis of $Fe(CO)_2(NO)_2$ dissolved in liquefied Krypton doped with 2% N_2. Initially (spectrum a), there are no bands in the N–N

Table I. Observed Wavenumbers (cm^{-1}) of $Fe(CO)_{2-x}(N_2)_x(NO)_2$ Species in Liquid Krypton Solution and Solid N_2 Matrices and Force Constants (N m^{-1})

liquid Kr (155 K)	calcd[a]	N_2 matrix[b] (10 K)	assgnt[c]
	$Fe(CO)_2(NO)_2$		
2086.9	2087.1	[2090, 2081]	a_1 ν_{C-O}
2038.5	2038.0	[2041, 2038]	b_1 ν_{C-O}
1817	1816.8	[1820, 1817]	a_1 ν_{N-O}
1775.8	1774.8	[1779, 1775]	b_2 ν_{N-O}
2073.1[d]	2073.0		a′ ν^{13}_{C-O}
2006.5[d]	2006.1		a″ ν^{13}_{C-O}
1805.3[d]	1806.1		a′ ν^{15}_{N-O}
1751.7[d]	1753.4		a″ ν^{15}_{N-O}
	$Fe(CO)(N_2)(NO)_2$		
2257.5		[2270, 2268, 2262]	a′ ν_{N-N}
2046.0		[2054, 2050, 2048]	a′ ν^{12}_{C-O}
2001.0[d,e]			a′ ν^{13}_{C-O}
1805.1		[1806, 1804]	a′ ν_{N-O}
1761.5		[1762, 1760]	a″ ν_{N-O}
	$Fe(N_2)_2(NO)_2$		
2250.5		2256[f]	a_1 ν_{N-N}
2228.0		2241[f]	b_1 ν_{N-N}
1796.3		[1795, 1792]	a_1 ν_{N-O}
1749.4		[1750, 1748]	b_2 ν_{N-O}

	$Fe(CO)_2(NO)_2$[g]	$Fe(CO)(N_2)(NO)_2$[g]	$Fe(N_2)_2(NO)_2$[g]
k_{NN}		2104	2071
k_{N_2,N_2}			21
k_{CO}	1718.7	1694	
$k_{CO,CO}$	40.9		
k_{NO}	1418.9	1401	1385
$k_{NO,NO}$	33.2	34	36

[a] Calculated by using the force constants tabulated below. Force constants were optimized with a "least-squares" refinement.[7] A more complete force constant analysis has been performed by Poletti et al.[5] [b] Taken from ref 4; bands assigned to matrix splittings bracketed together. [c] On the basis of C_{2v} symmetries for $Fe(CO)_2(NO)_2$ and $Fe(N_2)_2(NO)_2$ and C_s symmetry for $Fe(CO)(N_2)(NO)_2$. [d] Natural-abundance ^{13}C and ^{15}N. [e] $\nu^{12}_{C-O} - \nu^{13}_{C-O} = 45.0$ cm^{-1} (observed), 45.6 cm^{-1} (predicted). [f] Exact matrix band positions are uncertain because of the weakness of the bands. [g] Calculated assuming no vibrational coupling between N-N, C-O, and N-O groups.

(1) (a) Maier, W. B., II; Poliakoff, M.; Simpson, M. B.; Turner, J. J. *J. Chem. Soc., Chem. Commun.* **1980**, 587. (b) Turner, J. J.; Simpson, M. B.; Poliakoff, M.; Maier, W. B., II; Graham, M. A. *Inorg. Chem.* **1983**, *22*, 911.

(2) Turner, J. J.; Simpson, M. B.; Poliakoff, M.; Maier, W. B., II. *J. Mol. Struct.* **1982**, *80*, 83; *J. Am. Chem. Soc.* **1983**, *105*, 3898.
(3) Basolo, F. *Inorg. Chim. Acta* **1981**, *50*, 65.
(4) Crichton, O.; Rest, A. J. *J. Chem. Soc., Dalton Trans.* **1977**, 656.
(5) Poletti, A.; Santucci, A.; Foffani, A. *J. Mol. Struct.* **1969**, *3*, 311.

0020-1669/84/1323-0630$01.50/0